Combined Robust Design and Robust Control of an Electric DC Motor

Sulaiman F. Alyaqout, Panos Y. Papalambros, and A. Galip Ulsoy

***Abstract*—System performance can significantly benefit from optimally integrating the design and control of engineering systems. To improve the robustness properties of systems, this paper introduces an approach that combines robust design with robust control and investigates the coupling between them. However, the computational cost of improving this robustness can often be high due to the need to solve a resulting minimax design and control optimization problem. To reduce this cost, sequential and iterative strategies are proposed and compared to an all-in-one (Aio) strategy for solving the minimax problem. These strategies are then illustrated for a case study: Robust design and robust control (RDRC) of a dc motor. Results show that the resulting strategies can improve the robustness properties of the dc motor. In addition, the coupling strength between the robust design and robust control tends to increase as the applied level of uncertainty increases.**

***Index Terms*—Combined design and control, coupling, robust control, robust design.**

I. Introduction

INTEGRATING the design and control of engineering systems can result in improved performance for practical problems, such as vehicle suspensions [1], flexible structures [2]–[4], robotics [5], and electrical motors [6]. Traditionally, the design and control of such systems have been performed using sequential strategies that involve optimizing the design first and then optimizing the control. Utilizing system-level strategies, which guarantee optimality of the combined design and control optimization problem, resulted in improved performance compared to these sequential strategies. This result has been both proved theoretically and validated experimentally [1], [3], [6]–[9]. Interestingly, most integrated design and control formulations ignore the effect of control on design. However, Reyer's [6] work is an exception and incorporates control-related criteria in the design optimization problem.

Solving combined design and control optimization problems has received substantial attention from the researchers [10]. Fathy *et al.* [1], [11] introduced a system-level approach to solving the combined design and control optimization problem and compared his system-level approach to several other optimization strategies. Tanaka and Sugie [12] proposed a general formulation to the combined structure and control optimization problem and reduced the formulation to a bilinear matrix inequality (BMI) using a descriptor form; he also proposed an algorithm to solve the optimization problem. Yan and Yan [13] presented an integrated design and control approach to design a four-bar linkage driven by a servo motor. In contrast, iterative redesign strategies proposed by Skelton *et al.* [14], [15] have the advantage of guaranteeing a locally convergent solution to the optimization problem. Grossard *et al.* [16] investigated the design and control of piezoactive compliant micromechanisms using an evolutionary approach. Cakmakci and Ulsoy [17] presented a control formulation for networked control systems that maximizes component-swapping modularity and then demonstrated his approach with an example of driveshaft speed control with a dc motor.

While progress has been made toward solving integrated design and control optimization problems, the effects of uncertainty have not yet been considered. In practice, uncertainties are generated by modeling errors, payload variations, external disturbances, etc. Such undesirable factors can cause performance degradation when conventional control laws are applied. To deal with this uncertainty, many modern control techniques, such as fuzzy control [18], [19], variable structure control [20], adaptive control [21]–[23], fault-tolerant control [24], and nonlinear control [25], [26], have been proposed. However, such research in modern control of motors has been concerned with robust control. Robust control assumes that design (or plant) variables are considered as parameters and should not be modified during the controller design optimization process. Therefore, the effect of the design variables in improving the robustness of the control system has been ignored.

Several authors have examined strength-based coupling between design and control systems [3], [7], [27]. Reyer *et al.* [9] and Fathy *et al.* [11] proposed the use of optimality conditions to characterize coupling. They defined coupling relative to the solution method, for example, by comparing the optimality conditions of a sequential strategy with the optimality conditions of the system-level strategy. However, their work has considered design and control problems that do not incorporate uncertainty. By failing to incorporate uncertainty, the previous contributions did not discover any relationship between the applied level of uncertainty and the coupling measure. The main contribution of this paper is to introduce a combined design and control formulation that incorporates this uncertainty. Such a formulation can be used to examine the relationship between the coupling measure and uncertainty.

Manuscript received October 8, 2009; revised February 16, 2010; accepted March 6, 2010. Date of publication May 10, 2010; date of current version May 6, 2011. Recommended by Technical Editor J. Xu.

S. F. Alyaqout is with the Department of Mechanical Engineering, Kuwait University, Safat 13060, Kuwait (e-mail: s.alyaqout@ku.edu.kw).

P. Y. Papalambros and A. G. Ulsoy are with the Department of Mechanical Engineering, The University of Michigan, Ann Arbor, MI 48109-2125 USA (e-mail: pyp@umich.edu; ulsoy@umich.edu).

Color versions of one or more of the figures in this paper are available online at http://ieeexplore.ieee.org.

Digital Object Identifier 10.1109/TMECH.2010.2047652

This paper examines the robust design and robust control (RDRC) of a dc motor. This leads to establishing a relationship between the level of uncertainty and the coupling strength between the robust design and robust control. Section II poses the combined robust design robust control system problem under consideration. Section III describes how this combined system formulation can be applied to the RDRC of a dc motor. Section IV presents several optimization strategies to solve the RDRC dc motor problem. Then, Section V presents the numerical optimization results. Finally, Section VI concludes the paper with a discussion of results and future work.

II. RDRC Optimization Problem

We consider a general formulation that combines the robust design and robust control optimization problems. The formulation optimizes the combined design and control objective function in the presence of uncertainty (performance robustness) while maintaining constraint feasibility also in the presence of uncertainty (feasibility robustness).

The RDRC optimization problem is stated as follows:

$$\min_{\bar{\mathbf{x}},\mathbf{y}_{21},\mathbf{y}_{12}} \max_{\Delta\bar{\mathbf{x}},\hat{\mathbf{y}}_{12},\hat{\mathbf{y}}_{21}} F = w_d F_d(\hat{\mathbf{x}}_d,\hat{\mathbf{p}}_d,\hat{\mathbf{y}}_{21}) + w_c F_c(\mathbf{x}(t),\mathbf{u}(t),t,\hat{\mathbf{p}}_c,\hat{\mathbf{y}}_{12})$$

subject to

$$\dot{\mathbf{x}}(t) = r(\mathbf{x}(t),\mathbf{u}(t),t,\hat{\mathbf{x}}_d,\hat{\mathbf{p}}_d,\hat{\mathbf{p}}_c,\hat{\mathbf{y}}_{12})$$

$$\mathbf{h}_d(\hat{\mathbf{x}}_d,\hat{\mathbf{p}}_d,\hat{\mathbf{y}}_{21}) = \mathbf{0}\ ,\ \mathbf{h_c}(\mathbf{x}(t),\mathbf{u}(t),t,\hat{\mathbf{x}}_d,\hat{\mathbf{p}}_d,\hat{\mathbf{p}}_c,\hat{\mathbf{y}}_{12}) = \mathbf{0}$$

$$(\bar{\mathbf{x}}^T,\Delta\bar{\mathbf{x}}^T) \in \{(\bar{\mathbf{x}}^T,\Delta\bar{\mathbf{x}}^T) \in \mathbb{R}^{1\times(n_{\bar{\mathbf{x}}}+n_{\Delta\bar{\mathbf{x}}})} :$$

$$(\mathbf{1}-\beta_d)\cdot\mathbf{g}_d(\mathbf{x}_d,\mathbf{p}_d,\mathbf{y}_{21}) + \boldsymbol{\beta}_d\cdot\mathbf{g}_d(\hat{\mathbf{x}}_d,\hat{\mathbf{p}}_d,\hat{\mathbf{y}}_{21}) \le \mathbf{0},$$

$$(\mathbf{1}-\beta_c)\cdot\mathbf{g}_c(\mathbf{x}(t),\mathbf{u}(t),t,\mathbf{x}_d,\mathbf{p}_c,\mathbf{y}_{12}) + \boldsymbol{\beta}_c\cdot\mathbf{g}_c(\mathbf{x}(t),\mathbf{u}(t),t,\hat{\mathbf{x}}_d,\hat{\mathbf{p}}_c,\hat{\mathbf{y}}_{12}) \le \mathbf{0},$$

$$\text{for every}\ \ \Delta\bar{\mathbf{x}} \in \{\Delta\bar{\mathbf{x}} \in \mathbb{R}^{n_{\Delta\bar{\mathbf{x}}}} :\ \mathbf{g}_{\bar{\mathbf{x}}}(\Delta\bar{\mathbf{x}},\boldsymbol{\alpha}_{\bar{\mathbf{x}}}) \le \mathbf{0}\}\}$$

$$\mathbf{g}_{\bar{\mathbf{x}}}(\Delta\bar{\mathbf{x}},\boldsymbol{\alpha}_{\bar{\mathbf{x}}}) \le \mathbf{0},\ \ \mathbf{y}_{12} - Y_{12}(\mathbf{x}_d,\mathbf{p}_d,\mathbf{y}_{21}) = \mathbf{0}$$

$$\mathbf{y}_{21} - Y_{21}(\mathbf{x}(t),\mathbf{u}(t),t,\mathbf{p}_c,\mathbf{y}_{12}) = \mathbf{0}$$

$$\hat{\mathbf{y}}_{12} - \hat{Y}_{12}(\hat{\mathbf{x}}_d,\hat{\mathbf{p}}_d,\hat{\mathbf{y}}_{21}) = \mathbf{0}$$

$$\hat{\mathbf{y}}_{21} - \hat{Y}_{21}(\mathbf{x}(t),\mathbf{u}(t),t,\hat{\mathbf{p}}_c,\hat{\mathbf{y}}_{12}) = \mathbf{0} \tag{1a}$$

where

$$\bar{\mathbf{x}} \triangleq (\,\mathbf{x}_d^T,\mathbf{x}^T(t),\mathbf{u}^T(t)\,)^T\ ,\Delta\bar{\mathbf{x}} \triangleq (\,\Delta\mathbf{x}_d^T,\Delta\mathbf{p}_d^T,\Delta\mathbf{p}_c^T\,)^T$$

$$\hat{\mathbf{x}}_d = f_{\mathbf{x}_d}(\mathbf{x}_d,\Delta\mathbf{x}_d), \qquad \hat{\mathbf{p}}_d = f_{\mathbf{p}_d}(\mathbf{p}_d,\Delta\mathbf{p}_d) \tag{1b}$$

$$\hat{\mathbf{p}}_c = f_{\mathbf{p}_c}(\mathbf{p}_c,\Delta\mathbf{p}_c) \tag{1c}$$

and $\mathbf{x}(t) \in \mathbb{R}^n$ is the column vector of system state variables, $\mathbf{u}(t) \in \mathbb{R}^m$ is the control input, $\mathbf{x}_d \in \mathbb{R}^{n_{x_d}}$ is the column vector of design variables, $\mathbf{p}_d \in \mathbb{R}^{n_{p_d}}$ is the vector of design parameters, $\mathbf{p}_c \in \mathbb{R}^{n_{p_c}}$ is the vector of control parameters, $\bar{\mathbf{x}} \in \mathbb{R}^{n_{\bar{\mathbf{x}}}}$ is the vector of combined optimization variables, where $n_{\bar{\mathbf{x}}} = n_{x_d} + n + m$, $\mathbf{y}_{12} \in \mathbb{R}^{n_{y_d}}$ is the vector of interaction variables from design (system 1) to control (system 2), and $\mathbf{y}_{21} \in \mathbb{R}^{n_{y_c}}$ is the vector of interaction variables from control (system 2) to design (system 1). In addition, $F_d \in \mathbb{R}$, $F_c \in \mathbb{R}$ are the objective function representing the design and control performance, respectively; $\mathbf{g}_d \in \mathbb{R}^{n_{g_d}}$, $\mathbf{h}_d \in \mathbb{R}^{n_{h_d}}$ represent the design constraints, while $\mathbf{g}_c \in \mathbb{R}^{n_{g_c}}$, $\mathbf{h}_c \in \mathbb{R}^{n_{h_c}}$ represent the control constraints. Furthermore, $(.)^T$ is the vector transpose, $\cdot$ is the dot product, and $\triangleq$ represents a definition.

Several assumptions are associated with the RDRC formulation. The RDRC formulation is a worst case approach as represented by the minimax formulation in (1a). We assume real set-based uncertainty $\Delta\mathbf{x}_d \in \mathbb{R}^{n_{x_d}}$, $\Delta\mathbf{p}_d \in \mathbb{R}^{n_{p_d}}$, $\Delta\mathbf{p}_c \in \mathbb{R}^{n_{p_c}}$ resulting from variation in the design variables $\mathbf{x}_d$, the design parameters $\mathbf{p}_d$, and the control parameters $\mathbf{p}_c$, respectively. Note that in the problem statement above, all the uncertainty is parametric; no model uncertainty, which often results from model reduction, is included in the RDRC formulation.

Furthermore, the functions $f_{\mathbf{x}_d}$, $f_{\mathbf{p}_d}$, $f_{\mathbf{p}_c}$ with resulting variables $\hat{\mathbf{x}}_d \in \mathbb{R}^{n_{x_d}}$, $\hat{\mathbf{p}}_d \in \mathbb{R}^{n_{p_d}}$, $\hat{\mathbf{p}}_c \in \mathbb{R}^{n_{p_c}}$ defined in (1b) and (1c) represent the assumed type of uncertainty (additive, percentage) associated with design variables $\mathbf{x}_d$, design parameters $\mathbf{p}_d$, control parameters $\mathbf{p}_c$, respectively. For example, the uncertainty $\Delta\mathbf{x}_d$ can represent a 50% increase (i.e., $\Delta\mathbf{x}_d = 1.5$), while the variable $\hat{\mathbf{x}}_d$ represents the actual variable change $\hat{\mathbf{x}}_d = 1.5\mathbf{x}_d$. In addition, $\Delta\bar{\mathbf{x}} \in \mathbb{R}^{n_{\Delta\bar{\mathbf{x}}}}$ is the vector of combined uncertainty variables, where $n_{\Delta\bar{\mathbf{x}}} = n_{x_d} + n_{p_d} + n_{p_c}$, $\hat{\mathbf{y}}_{12} \in \mathbb{R}^{n_{y_d}}$, $\hat{\mathbf{y}}_{21} \in \mathbb{R}^{n_{y_c}}$ represent the uncertain interaction variables associated with $\mathbf{y}_{12}$, $\mathbf{y}_{21}$, respectively. The $\boldsymbol{\alpha}_{\bar{\mathbf{x}}} \in \mathbb{R}^{n_{\Delta\bar{\mathbf{x}}}}$ is the level of uncertainty in design variables, design parameters, and control parameters. The $\boldsymbol{\alpha}_{\bar{\mathbf{x}}}$ and the inequality constraint $\mathbf{g}_{\bar{\mathbf{x}}} \in \mathbb{R}^{n_{g_{\bar{\mathbf{x}}}}}$ are used to define the uncertainty set. The final assumption is the transformation of the multiobjective optimization problem into a linear scalar substitute objective function using the design, control weights $w_d, w_c \in \mathbb{R}$, respectively. This choice of scalarization achieves the true Pareto curve only for a convex Pareto set, but it is used here for simplicity.

Feasibility robustness using a worst case approach could lead to an overly conservative design. To alleviate this conservatism, we propose utilizing the parameters $\boldsymbol{\beta}_d$, $\boldsymbol{\beta}_c$ in (1a) to vary the level of feasibility robustness, where $\boldsymbol{\beta}_d \in \{\boldsymbol{\beta} \in \mathbb{R}^{n_{g_d}} | \mathbf{0} \le \boldsymbol{\beta} \le \mathbf{1}\}$ and $\boldsymbol{\beta}_c \in \{\boldsymbol{\beta} \in \mathbb{R}^{n_{g_c}} | \mathbf{0} \le \boldsymbol{\beta} \le \mathbf{1}\}$. The physical interpretation of utilizing $\boldsymbol{\beta}_d$, $\boldsymbol{\beta}_c$ to vary feasibility robustness is illustrated on the single inequality constraint in Fig. 1. Consider setting $\boldsymbol{\beta}_d = \mathbf{0}$. Then the constraints will be satisfied only at the nominal design values and the system is not robustly feasible. Now consider setting $\boldsymbol{\beta}_d = \mathbf{1}$. Then the constraints will be satisfied at the worst case design values and the system is robustly feasible because the inequality constraint will always be satisfied even when subjected to uncertainty. Requiring $\boldsymbol{\beta}$ to be a unit vector tends to be extremely conservative because the worst case is unlikely to occur. The $\boldsymbol{\beta}$ level provides a means to ease this conservatism by providing the designer with a method of choosing the level of feasibility robustness.

There are several challenges associated with solving the RDRC optimization problem. The solution requires heavy computational effort even for modestly sized problems, since the

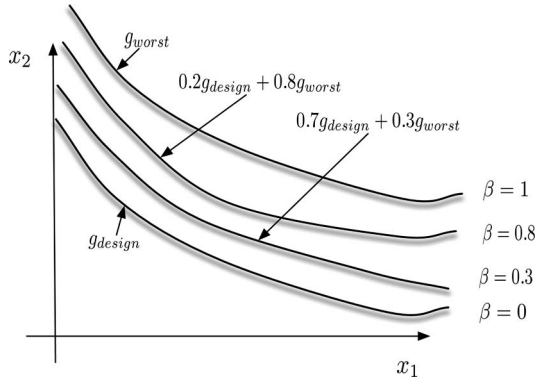

Fig. 1. Varying feasibility robustness using β.

number of design variables under uncertainty increases the complexity of the optimization problem. In addition, the RDRC can be a nonconvex optimization problem even if the individual RDRC optimization problems are convex. These issues will be further discussed in Section IV. However, application of RDRC to a dc motor is first presented in Section III.

III. Robust DC Motor Optimization Problem

The RDRC of a dc motor is presented in this section. The design determines the rotor dimensions and winding characteristics, while the control determines the input voltage to control the rotational response of the rotor. The objective is to improve performance robustness of a weighted sum of motor weight, system response, and control effort, while maintaining feasibility robustness of thermal limitations and geometric limitation. We first introduce the robust design problem, then the robust control problem, and finally, we combine the two problems to yield the RDRC.

A. Robust Design Problem

The design problem optimizes the static characteristics of the motor. The design objective is to minimize the worst case motor weight, while maintaining constraint feasibility for configuration (windings, magnetic fields) constraints and service requirements (speed, power) constraints. We utilize the design model system equations introduced by Reyer and Papalambros [6] to define the following robust design problem:

$$\min_{D,d_s,L,L_{wa},L_{wf}} \max_{\substack{\Delta D,\Delta L,\Delta A_{wa} \\ (\hat{v}_{\max},\hat{n}_{\max},\hat{p}_{\min},\hat{t}_{\min})\in\mathbb{S}_d}} F_d = \rho_{\mathrm{cu}}(\hat{A}_{wa}L_{wa} + A_{wf}L_{wf}) + \rho_{\mathrm{fe}}\hat{L}\,\pi(\hat{D}+d_s)^2$$

subject to

$$h_1 = ac - \frac{2\hat{p}_{\min}L_{wa}}{\pi\eta\, a\hat{v}_{\max}(2\hat{L} + \frac{2.3\pi\hat{D}}{p} + 5d_s)\hat{D}}$$

$$h_2 = I_f - \frac{A_{wf}^2\hat{v}_{\max}}{h_f L_{mtf} b_{fc} f_{cf} p\rho} \quad , \quad h_3 = B_g - \mathrm{func}(ac)$$

$$h_4 = L_{mtf} - \left(\hat{L} + 2b_{fc} + \frac{\psi}{\hat{L}}\right) \quad , \quad h_5 = h_f - \frac{0.76\psi}{\hat{L}}$$

$$(\mathbf{x}_d^T, \Delta\mathbf{x}_d^T, \Delta\mathbf{p}_d^T, \hat{\mathbf{y}}_{21}^T) \in \{(\mathbf{x}_d^T, \Delta\mathbf{x}_d^T, \Delta\mathbf{p}_d^T, \hat{\mathbf{y}}_{21}^T) \in \mathbb{R}^{1\times 12} :$$

$$g_1 = \frac{\pi\hat{D}}{p} - 0.38, \qquad g_2 = \frac{2\hat{D}B_g}{(\hat{D}-2d_s)} - 1.8$$

$$g_3 = \frac{\pi\hat{D}}{\hat{n}_{\max}} - 25, \qquad g_4 = 8 - \frac{\pi\hat{D}}{\hat{n}_{\max}}$$

$$g_5 = \frac{\hat{L}p}{\pi\hat{D}} - 0.9, \qquad g_6 = 0.6 - \frac{\hat{L}p}{\pi\hat{D}}$$

$$g_7 = \frac{2\hat{D}}{(\hat{D}-2d_s)} - 3.5, \qquad g_8 = 2.5 - \frac{2\hat{D}}{(\hat{D}-2d_s)}$$

$$g_9 = B_g - 0.8, \qquad g_{10} = 0.3 - B_g$$

$$g_{11} = d_s - \frac{2\pi(\hat{D}-2d_s)}{S}, \qquad g_{12} = d_s - 0.5\hat{D}$$

$$g_{13} = ac - 20, \qquad g_{14} = 6 - ac$$

$$g_{15} = \hat{p}_{\min} - \pi^2\psi B_g ac\hat{D}^2\hat{L}\,\hat{n}_{\max}$$

$$g_{16} = \hat{t}_{\min} - \frac{\pi}{2}\psi B_g ac\hat{D}^2\hat{L}$$

$$g_{17} = \frac{1.2L_{wa}\hat{A}_{wa}}{2\hat{L} + 2.3\frac{\pi\hat{D}}{p} + 5d_s} - \pi\frac{\hat{D}}{4}^2 + \pi\left(\frac{\hat{D}}{2} - d_s\right)^2$$

$$g_{18} = 500 - \frac{I_f^2 L_{wf}\rho}{A_{wf}(L_{mtf} + b_{fc})h_f}$$

$$g_{19} = \frac{I_f^2 L_{wf}\rho}{A_{wf}(L_{mtf} + b_{fc})h_f} - 750$$

$$\text{for every } \Delta\bar{\mathbf{x}} \in \{\Delta\bar{\mathbf{x}} \in \mathbb{R}^3 : (\Delta D, -\Delta D, \Delta L, -\Delta L, \Delta A_{wa}, -\Delta A_{wa})^T \le \boldsymbol{\alpha}_{\bar{\mathbf{x}}}\},\ \hat{\mathbf{y}}_{21} \in \mathbb{S}_d\}$$

$$(\Delta D, -\Delta D, \Delta L, -\Delta L, \Delta A_{wa}, -\Delta A_{wa})^T \le \boldsymbol{\alpha}_{\bar{\mathbf{x}}} \qquad (2)$$

where

$$\hat{D} = (\Delta D)D, \qquad \hat{L} = (\Delta L)L, \quad \hat{A}_{wa} = (\Delta A_{wa})A_{wa}.$$

The design variables are rotor diameter D, depth of slots d_s, rotor axial length L, length of armature wire L_{wa}, and length of field wire L_{wf}. The design parameters are resistivity ρ, depth of field coil b_{fc}, copper space factor f_{cf}, number of slots S, number of poles p, pole arc to pole pitch ratio ψ, motor efficiency η, number of paths a, cross-sectional area of wires A_{wa}, A_{wf}, and densities of copper and iron $\rho_{\mathrm{cu}}, \rho_{\mathrm{fe}}$, respectively. Moreover, the specific electrical loading ac, field current I_f, field winding height h_f, mean turn length of field coil L_{mtf}, and the maximum flux density B_g are functions of design variables as described by Hamdi [28].

We assume the percentage type uncertainty ΔD, ΔL, ΔA_{wa} resulting from variation in the rotor diameter D, the rotor axial length L, and the cross-sectional area of armature design parameter A_{wa}, respectively. $\mathbb{S}_d$ is the uncertainty set that results from propagating the uncertainty associated with interaction pa-

rameters $\hat{v}_{\max}, \hat{n}_{\max}, \hat{p}_{\min}, \hat{t}_{\min}$ from the control problem to the design problem. The robust control problem relationships are

$$\begin{aligned}
\hat{R}_a &= \frac{\rho L_{wa}}{4\hat{A}_{wa}} \\
\hat{K}_m &= K_m(\hat{D}, \hat{L}, L_{wa}, L_{wf}, \hat{v}_{\max}, p, \hat{A}_{wa}, A_{wf}) \\
\hat{L}_a &= \frac{\pi\psi\mu_0 L_{wa}^2 \hat{D}\hat{L}}{0.025\pi\hat{D}\left(2\hat{L} + \frac{2.3\pi\hat{D}}{p} + 5d_s\right)^2} \\
\hat{J}_a &= 0.5\pi\rho_{\text{fe}}\hat{L}\left(\frac{\hat{D}}{2} - d_2\right)^2 \\
&\quad + 0.5\rho_{\text{cu}} L_{wa} A_{wa}\left(\left(\frac{\hat{D}}{2}^2\right) - \left(\frac{\hat{D}}{2} - d_s\right)^2\right) \quad (3)
\end{aligned}$$

where the interaction parameters are armature resistance $\hat{R}_a$, motor constant $\hat{K}_m$ [28], armature inductance $\hat{L}_a$, and rotor inertia $\hat{J}_a$.

Now let us write the dc motor robust design problem in terms of the RDRC notation introduced in (1a). The design variables are $\mathbf{x}_d = (D, d_s, L, L_{wa}, L_{wf})^T$, design parameters are $\mathbf{p}_d = (S, \rho_{\text{cu}}, \rho_{\text{fe}}, A_{wf}, A_{wa}, a, \eta, b_{fc}, f_{cf}, p, \rho, \psi)^T$, design variable uncertainty is $\Delta\mathbf{x}_d = (\Delta D, \Delta L)^T$, design parameter uncertainty is $\Delta\mathbf{p}_d = (\Delta A_{wa})^T$, combined uncertainty variables are $\Delta\bar{\mathbf{x}} \triangleq (\Delta\mathbf{x}_d^T, \Delta\mathbf{p}_d^T)^T$, interaction parameters sent to the robust control problem are $\hat{Y}_{12} = (\hat{R}_a, \hat{K}_m, \hat{L}_a, \hat{J}_a)^T$, and interaction parameters arriving from the robust control problem are $\hat{\mathbf{y}}_{21} = (\hat{v}_{\max}, \hat{n}_{\max}, \hat{p}_{\min}, \hat{t}_{\min})^T$. Note that the interaction variables $\hat{\mathbf{y}}_{21}$ in (1a) are now the parameters in the robust control problem, hence the term "interaction parameters."

B. Robust Control Problem

The controller location and how the motor is wound directly affect the form of the dc motor controller. We assume a proportional plus integral plus derivative (PID) controller configuration for the armature-controlled motor. The robust control problem can be stated as

$$\min_{K_p, K_i, K_d} \max_{(\hat{r}_a, \hat{k}_m, \hat{l}_a, \hat{j}_a) \in \mathbb{S}_c} F_c = \int_0^{t_f} e(t)^T Q e(t) dt + \hat{V}_{\max}$$

subject to

$$\frac{d}{dt}\begin{bmatrix} i \\ \omega \end{bmatrix} = \begin{bmatrix} \frac{-\hat{r}_a}{\hat{l}_a} & \frac{-\hat{k}_m}{\hat{l}_a} \\ \frac{\hat{k}_m}{\hat{j}_a} & \frac{B}{\hat{j}_a} \end{bmatrix}\begin{bmatrix} i \\ \omega \end{bmatrix} + \begin{bmatrix} \frac{1}{\hat{l}_a} \\ 0 \end{bmatrix} u(t) + \begin{bmatrix} 0 \\ \frac{-1}{\hat{j}_a} \end{bmatrix} \tau_L$$

$$u(t) = K_p\, e(t) + K_i \int e(t)dt + K_d \frac{de(t)}{dt} \quad (4)$$

where

$$y(t) = \omega(t), \qquad e(t) = y(t) - y_d(t)$$

where the robust control variables are proportional gain K_p, integral gain K_i, and derivative gain K_d. The parameters are friction coefficient B and regulator weight Q. $\mathbb{S}_c$ is the uncertainty set that results from propagating the uncertainty associated with interaction parameters $\hat{r}_a, \hat{k}_m, \hat{l}_a, \hat{j}_a$ from the design problem to the control problem. The control signals are angular velocity of rotor $\omega(t)$, current $i(t)$, input voltage $u(t)$, and applied load torque τ_L [6]. The robust design problem quantities are the following:

$$\begin{aligned}
&\hat{V}_{\max} = \max_t(u(t)), \qquad \hat{N}_{\max} = \max_t(\omega(t)), \\
&\hat{P}_{\min} = \max_t(u(t)i(t)), \qquad \hat{T}_{\min} = \max_t(\hat{k}_m i(t) - \tau_L(t)).
\end{aligned} \quad (5)$$

Now let us write the dc motor robust control problem in terms of the RDRC notation introduced in (1a). The control problem variables are $\boldsymbol{K} = (K_p, K_i, K_d)^T$, control parameters are $\mathbf{p}_c = (B, Q)^T$, interaction parameters sent to the robust design problem are $\hat{Y}_{21} = (\hat{V}_{\max}, \hat{N}_{\max}, \hat{P}_{\min}, \hat{T}_{\min})^T$, and interaction parameters arriving from the robust design problem are $\hat{\mathbf{y}}_{12} = (\hat{r}_a, \hat{k}_m, \hat{l}_a, \hat{j}_a)^T$.

C. RDRC Optimization Problem

The RDRC problem combines the robust design problem in (2) with the robust control problem in (4). The $\boldsymbol{\beta}$ level is introduced to provide the designer with a method of choosing the desired level of feasibility robustness. The combined RDRC formulation for the dc motor can be written as follows:

$$\begin{aligned}
&\min_{\mathbf{x}_d, \boldsymbol{K}, \mathbf{y}_{12}, \mathbf{y}_{21}} \max_{\Delta\mathbf{x}_d, \Delta\mathbf{p}_d, \Delta\mathbf{p}_c, \hat{\mathbf{y}}_{12}, \hat{\mathbf{y}}_{21}} w_d\rho_{\text{cu}}(\hat{A}_{wa}L_{wa} + A_{wf}L_{wf}) \\
&\quad + w_d\rho_{\text{fe}}\hat{L}\pi(\hat{D} + d_s)^2 + w_c\left(\int_0^{t_f} e(t)^T Q e(t) dt + \hat{V}_{\max}\right)
\end{aligned}$$

subject to

$$\frac{d}{dt}\begin{bmatrix} i \\ \omega \end{bmatrix} = \begin{bmatrix} \frac{-\hat{r}_a}{\hat{l}_a} & \frac{-\hat{k}_m}{\hat{l}_a} \\ \frac{\hat{k}_m}{\hat{j}_a} & \frac{B}{\hat{j}_a} \end{bmatrix}\begin{bmatrix} i \\ \omega \end{bmatrix} + \begin{bmatrix} \frac{1}{\hat{l}_a} \\ 0 \end{bmatrix} u(t) + \begin{bmatrix} 0 \\ \frac{-1}{\hat{j}_a} \end{bmatrix} \tau_L$$

$$u(t) = K_p\, e(t) + K_i \int e(t)dt + K_d \frac{de(t)}{dt}$$

$$\begin{aligned}
&(\bar{\mathbf{x}}^T, \Delta\bar{\mathbf{x}}^T) \in \{(\bar{\mathbf{x}}^T, \Delta\bar{\mathbf{x}}^T) \in \mathbb{R}^{1\times(n_{\bar{\mathbf{x}}} + n_{\Delta\bar{\mathbf{x}}})} : \\
&(1 - \boldsymbol{\beta}_d)\cdot\mathbf{g}_d(\mathbf{x}_d, \mathbf{p}_d, \mathbf{y}_{21}) + \boldsymbol{\beta}_d \cdot \mathbf{g}_d(\hat{\mathbf{x}}_d, \hat{\mathbf{p}}_d, \hat{\mathbf{y}}_{21}) \le \mathbf{0} \\
&\quad \text{for every } \Delta\bar{\mathbf{x}} \in \{\Delta\bar{\mathbf{x}} \in \mathbb{R}^{n_{\Delta\bar{\mathbf{x}}}} : \\
&(\Delta D, -\Delta D, \Delta L, -\Delta L, \Delta A_{wa}, -\Delta A_{wa})^T \le \boldsymbol{\alpha}_{\bar{\mathbf{x}}}\}\} \\
&\mathbf{h}_d = \mathbf{0}, \qquad \mathbf{y}_{12} - Y_{12} = \mathbf{0}, \qquad \mathbf{y}_{21} - Y_{21} = \mathbf{0} \\
&\hat{\mathbf{y}}_{12} - \hat{Y}_{12} = \mathbf{0}, \qquad \hat{\mathbf{y}}_{21} - \hat{Y}_{21} = \mathbf{0} \\
&(\Delta D, -\Delta D, \Delta L, -\Delta L, \Delta A_{wa}, -\Delta A_{wa})^T \le \boldsymbol{\alpha}_{\bar{\mathbf{x}}},
\end{aligned} \quad (6)$$

where

$$\begin{aligned}
&y(t) = \omega(t), \qquad e(t) = y(t) - y_d(t) \\
&\mathbf{h}_d = [h_1, h_2, \ldots, h_5]^T, \qquad \mathbf{g}_d = [g_1, g_2, \ldots, g_{19}]^T \\
&\mathbf{y}_{12} = (r_a, k_m, l_a, j_a)^T\ ,\ \mathbf{y}_{21} = (v_{\max}, n_{\max}, p_{\min}, t_{\min})^T
\end{aligned}$$

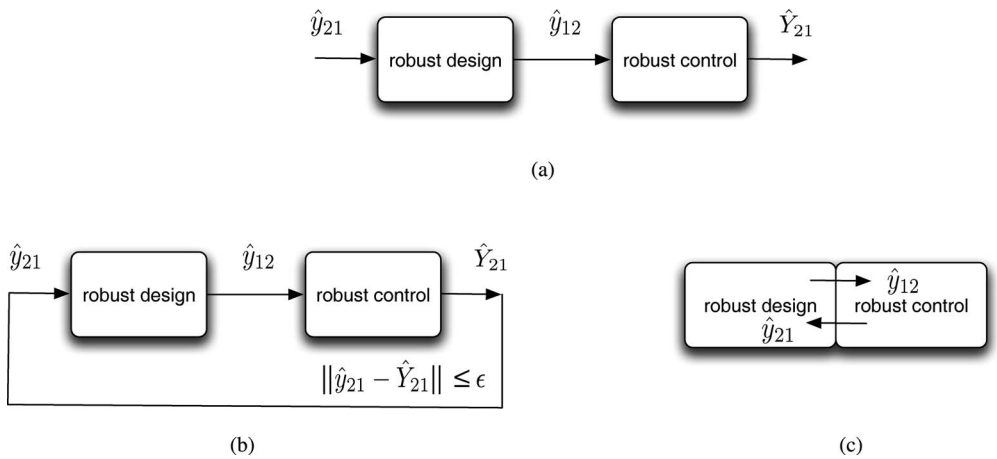

Fig. 2. Optimization strategies under uncertainty. (a) Sequential strategy. (b) Iterative strategy. (c) All-in-one strategy.

$Y_{12} = (R_a, K_m, L_a, J_a)^T, Y_{21} = (V_{\max}, N_{\max}, P_{\min}, T_{\min})^T$

$\hat{D} = (\Delta D)D, \qquad \hat{L} = (\Delta L)L, \qquad \hat{A}_{wa} = (\Delta A_{wa})A_{wa}$

where $R_a, K_m, L_a, J_a, V_{\max}, N_{\max}, P_{\min}, T_{\min}$ are defined similarly using (2)–(5) but without the hat $\hat{}$ symbol. Let us consider now how to solve this problem efficiently.

IV. Optimization Strategies

We consider several strategies used to solve the RDRC optimization problem. The strategies presented are classified into sequential or iterative strategies under uncertainty that solve separate RDRC optimization problems, and an all-in-one (Aio) strategy that solves the RDRC system problem.

A. Sequential Strategy Under Uncertainty

A sequential strategy under uncertainty solves the robust design first, then the robust control, as shown in Fig. 2(a). The sequential strategy starts by initializing the interaction parameter $\hat{\mathbf{y}}_{21}$, solves the robust design problem, uses the resulting solution to compute $\hat{\mathbf{y}}_{12}$, solves the robust control problem, and computes a new $\hat{Y}_{21}$. The robust design optimization problem requires an initial guess for the design variables and the robust control optimization problem requires an initial guess for the control variables. A sequential strategy represents the traditional way to solving design and robust control problems, by optimizing the design first and then either an optimal controller or a robust controller is sought. Although it is simple, the sequential strategy may suffer from inconsistency due to the mismatching of $\hat{\mathbf{y}}_{21}$ and $\hat{Y}_{21}$ or $\hat{\mathbf{y}}_{12}$ and $\hat{Y}_{12}$. Solution is dependent on initial guesses for the values of the interaction parameters.

B. Iterative Strategy Under Uncertainty

An iterative strategy under uncertainty solves the separate RDRC optimization problems repeatedly until convergence is achieved, as shown in Fig. 2(b). The sequential strategy starts by initializing the interaction parameter $\hat{\mathbf{y}}_{21}$. In addition, the robust design optimization problem requires an initial guess for the design variables and the robust control optimization problem requires an initial guess for the control variables. The iterative strategy updates the interaction parameters until convergence is achieved by matching the interaction parameters within some tolerance, namely, it terminates when $\|\hat{\mathbf{y}}_{21} - \hat{Y}_{21}\|_2 \leq \epsilon$, where ϵ is the prescribed tolerance. The iterative strategy is not guaranteed to converge to the solution and the computational cost may become high. However, with a good initial guess and enough iterations, the interaction parameters will become consistent.

C. All-in-One Strategy Under Uncertainty

The Aio strategy under uncertainty solves the RDRC directly and can achieve the system optimum. The interaction parameters $\hat{\mathbf{y}}_{21}, \hat{\mathbf{y}}_{12}$ become variables in the Aio strategy, so the optimizer handles consistency of the interactions, as shown in Fig. 2(c). The Aio strategy optimization problem requires an initial guess for the design variables, control variables, and interaction parameters. The Aio strategy must solve a larger optimization problem compared to sequential and iterative strategies; therefore, the strategy generally requires more computational effort. However, as noted, iterative strategies could require more computational effort than the Aio strategy if convergence requires a large number of iterations.

The RDRC problem in (6) imposes consistency of $\hat{\mathbf{y}}_{21}$ with $\hat{Y}_{21}$ and $\hat{\mathbf{y}}_{12}$ with $\hat{Y}_{12}$ using equality constraints. Reyer's [6] Aio strategy relaxes these equality constraints to inequality constraints. Here, we utilize equality constraints to define a coupling measure (Section V-B).

V. Simulation Results

We use the optimization strategies introduced in Section IV to solve the dc motor problem. We then examine the relationship between level of uncertainty and coupling strength between robust design and robust control.

A. Robust DC Motor Results

Optimization was performed with a sequential quadratic programming (SQP) algorithm. The MATLAB "fmincon"

TABLE I
RDRC STRATEGIES UNDER UNCERTAINTY

Description	Sequential		Iterative		All-in-One	
	nominal	robust	nominal	robust	nominal	robust
Nominal Objective, $5F_d$+$0.5F_c$	166.04	168.03	131.91	143.38	97.608	103.16
Worst Objective, 5 $max(F_d)$+0.5 $max(F_c)$	173.02	175.02	141.86	152.91	104.59	110.32
Weight (kg), F_d	24.587	24.852	16.465	17.948	12.076	12.393
Control Performance, F_c	86.206	87.543	99.162	107.27	74.457	82.391
Worst Weight (kg), $max(F_d)$	25.91	26.189	17.438	19.024	12.811	13.154
Worst Control Performance, $max(F_c)$	86.941	88.142	109.35	115.57	81.076	89.093
Rotor Diameter (cm), D	10.065	10.115	10.695	11.031	9.9947	10.045
Rotor Axial Length (cm), L	14.229	14.239	10.079	10.439	9.4198	9.5067
Armature Wire Length (m), L_{wa}	285.2	286.04	232.49	259.09	107.77	122.98
Field Wire Length (m), L_{wf}	653.53	658.44	302.58	268.58	268.28	232.37
Slot Depth (cm), d_s	1.5701	1.5731	2.0019	2.0586	1.8709	1.8747
Proportional Gain, K_p	1.4971	1.5027	1.704	1.9796	1.8845	2.1863
Integral Gain, K_i	9.0721	8.6733	5.4777	4.6579	10	10
Derivative Gain, K_d	0.0606	0.0632	0.0092	0.0083	0	0
Max Rotational Speed (rad/s), $\hat{n}_{max}$	30.811	30.811	23.81	23.272	25.478	25.505
$\hat{N}_{max}$	24.088	23.707	23.81	23.272	25.478	25.505
Max Voltage (V), $\hat{v}_{max}$	65.774	65.774	42.77	48.342	46.716	53.581
$\hat{V}_{max}$	37.967	37.731	42.77	48.342	46.716	53.581
Min Required Torque (Nm), $\hat{t}_{min}$	18.692	18.692	5.6922	5.691	6.1747	6.2276
$\hat{T}_{min}$	6.1109	6.022	5.6922	5.691	6.1747	6.2276
Min Required Power (kW), $\hat{p}_{min}$	0.901	0.9001	0.4016	0.4144	0.9884	1.0201
$\hat{P}_{min}$	0.185	0.178	0.4016	0.4144	0.9884	1.0201
Inductance (cH), $\hat{l}_a$	73.44	73.48	38.56	46.55	8.8665	11.52
$\hat{L}_a$	73.44	73.48	38.56	46.55	8.8665	11.52
Resistance (cΩ), $\hat{r}_a$	63.936	64.124	52.12	58.08	24.159	27.57
$\hat{R}_a$	63.936	64.124	52.12	58.08	24.159	27.57
Inertia (kg m^2), $\hat{j}_a$	0.0194	0.0198	0.0144	0.017	0.0077	0.0084
$\hat{J}_a$	0.0194	0.0198	0.0144	0.017	0.0077	0.0084
Motor constant, $\hat{k}_m$	1.0885	1.0943	0.436	0.4711	0.1963	0.2169
$\hat{K}_m$	1.0885	1.0943	0.436	0.4711	0.1963	0.2169
Computation Time (min)	0.2	0.6	6	105	12	30
Maximum Closed-loop Eigenvalue	-4.6544	-4.3723	-2.969	-2.0427	-5.3953	-4.5871

optimization routine utilizes SQP to search for the optimal values. Since SQP finds local optima, a multistarting point technique was employed in the search. These starting points included the values that result from the Aio strategy. We assume that the uncertainty variables $\Delta D, \Delta L$ and parameter ΔA_{wa} are bounded by the vector $\boldsymbol{\alpha}_{\bar{\mathbf{x}}} = (1.02, -1.02, 1.008, -1.008, 1.04, -1.04)^T$ to represent percentage type uncertainty as described in (2). Note that this represents 2% uncertainty in rotor diameter D, 0.8% uncertainty in rotor axial length L, and 4% uncertainty in the cross-sectional area of armature A_{wa}. In addition, we assume that the vector $\boldsymbol{\beta} = 0.15(\mathbf{1})$ maintains a level of feasibility robustness in the presence of uncertainty. The dc motor design parameters are $\mathbf{p}_d = (S, \rho_{\mathrm{cu}}, \rho_{\mathrm{fe}}, A_{wf}, A_{wa}, a, \eta, b_{fc}, f_{cf}, p, \rho, \psi)^T = (21, 8890, 7750, 0.5 \times 10^{-6}, 2 \times 10^{-6}, 2, 0.85, 40 \times 10^{-3}, 0.5, 2, 1.7241 \times 10^{-8}, 0.6667)^T$. The control parameters are $\mathbf{p}_c = (B, Q)^T = (0.23, 1)^T$.

The results of using the strategies from Section IV to solve the dc motor problem are presented in Table I. For each strategy, the first column ("nominal") represents the assumption of zero uncertainty for the optimization strategy. These points are often not feasibly robust because they fail to satisfy the constraints under uncertainty. While the second column ("robust") represents the robust points obtained using the optimization strategies with the above-assumed uncertainty.

The sequential strategy yielded the lowest robustness (the highest worst case performance) compared to the iterative and Aio strategies as shown in Table I. This strategy's results yielded large rotor axial length L, armature wire length L_{wa}, and field wire length L_{wf} compared to the iterative and Aio strategies. Moreover, the strategy results in a small proportional controller gain K_p and large derivative gain K_d compared to the iterative and Aio strategies. The sequential strategy under uncertainty seemed to increase the rotor axial length, the armature wire length, the field wire length, and the derivative gain even further compared to the sequential strategy with zero uncertainty. However, the sequential strategy has the advantage of extremely efficient computation time compared to the iterative and Aio strategies. On the other hand, the sequential strategy results are highly dependent on the assumed values of initial interaction parameters $\hat{\mathbf{y}}_{21}$. In addition, the sequential strategy is inconsistent since the max rotational speed, max voltage, min required

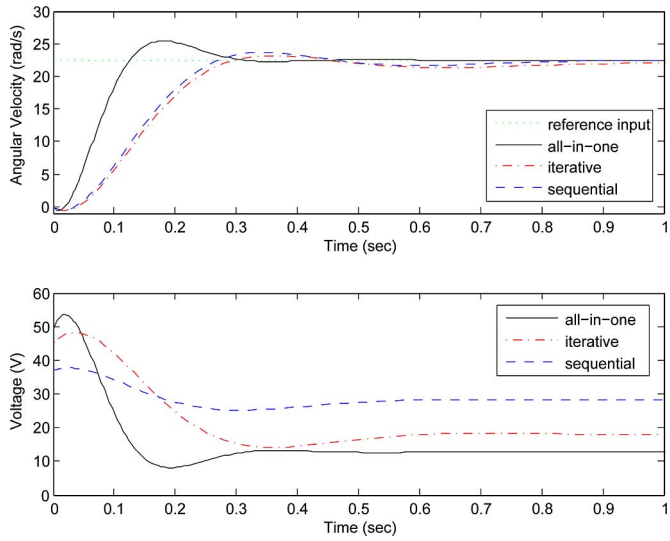

Fig. 3. Robust (zero uncertainty) dynamic response of the dc motor.

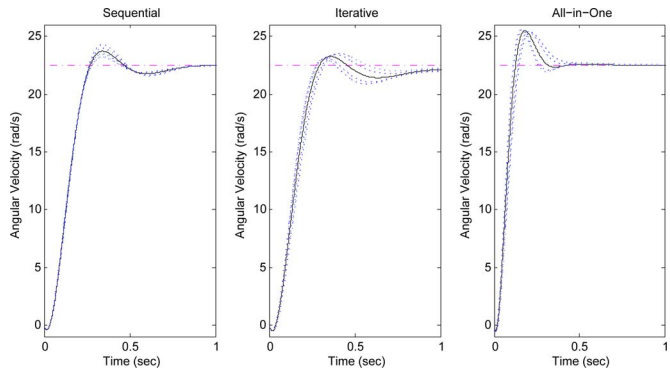

Fig. 4. Robust angular velocity response of the dc motor under uncertainty. Response to zero uncertainty (—), uncertainty between 0% and 20% ($\cdots$).

torque, and min required power are all inconsistent. The sequential approach solution is acceptable since it only requires satisfaction of an inequality constraint for the interaction parameters $\hat{n}_{\max}, \hat{N}_{\max}, \hat{v}_{\max}, \hat{V}_{\max}, \hat{t}_{\min}, \hat{T}_{\min}, \hat{p}_{\min}$, and $\hat{P}_{\min}$ [6]. On the other hand, the iterative strategy and Aio are consistent and enforce an equality constraint for the interaction parameters as shown in Table I. So the sequential strategy results are not directly comparable to the iterative and Aio strategies results shown in Table I or Figs. 3–5.

The iterative strategy yielded improved robustness compared to the sequential strategy as shown in Table I. The worst case objective of the iterative is 152.91, while the worst case objective of the sequential is 175.02. Based on our definition of robustness, the iterative strategy is more robust than the sequential strategy. However, the computational effort increased considerably as a result of incorporating uncertainty. The iterative strategy under uncertainty required 300 iterations for $\epsilon = 0.2$ (105 min), while the iterative strategy with zero uncertainty required only 68 iterations for $\epsilon = 0.2$ (6 min). Hence, by incorporating uncertainty, the computational effort not only increased in the design and control subproblems, but also convergence required more iterations. As for closed-loop stability, the iterative strategy seemed

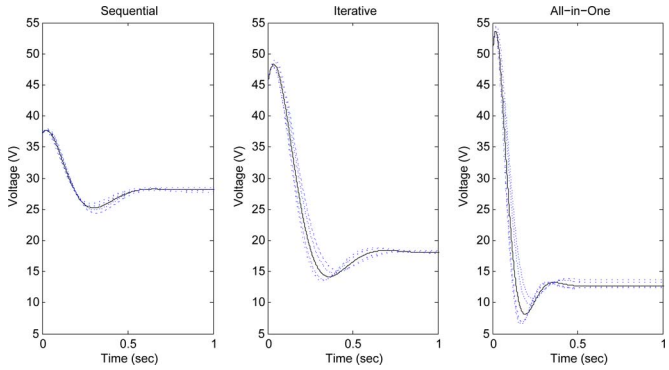

Fig. 5. Robust voltage response of the dc motor under uncertainty. Response to zero uncertainty (—), uncertainty between 0% and 20% ($\cdots$).

to have the worst relative stability (absolute value of maximum closed-loop eigenvalue) compared to the sequential and Aio strategies as shown in Table I. All the strategies under uncertainty seemed to yield points with the largest eigenvalue closer to instability (i.e., smaller relative stability) compared to strategies under no uncertainty (i.e., larger relative stability). This can be attributed to the fact that relative stability was not considered as an optimization criterion.

The Aio strategy yielded the best performance as shown in Table I. The robustness improvement of the Aio solution compared to the iterative and sequential strategies is substantial. The worst case objective of the Aio is 110.32, while the worst case objective of the iterative is 152.91. Based on our definition of robustness, the Aio strategy is more robust than the iterative strategy. The Aio worst design objective of 13.154 is a big improvement compared to the sequential worst design objective of 26.189. On the other hand, the worst control objective of the Aio strategy is almost identical to the worst control objective of the sequential strategy. A designer can improve further the Aio worst control objective, at the expense of increasing the worst design objective, by increasing the ratio of control weight over design weight w_c/w_d. However, the computational effort increased considerably as a result of incorporating uncertainty. The Aio strategy results yielded the smallest rotor diameter D, rotor axial length L, and armature wire length L_{wa} compared to the iterative and Aio strategies. Moreover, the strategy tended to increase the integral controller gain K_i and decrease the derivative gain K_d. Incorporating uncertainty increased the computational time considerably from 12 to 30 min. However, the iterative strategy's computational effort with 105 min remains larger than the computational effort of the Aio strategy. Note that the iterative strategy computational effort was lower compared to the Aio for nominal systems (zero uncertainty).

Fig. 3 compares the robust (zero uncertainty) dynamic response of the sequential, iterative, and Aio strategies. For the angular velocity response, the Aio strategy yielded a faster response but at the expense of some overshoot, while the sequential yielded a slightly faster response than the iterative. For the input voltage response, the Aio strategy reduced the control effort considerably, which explains the superior performance of the Aio. The sequential strategy required less maximum (or

peak) input voltage compared to the iterative and Aio strategies. The angular velocity transfer functions for all the strategies are nonminimum phase transfer functions because each has a zero in the right-hand plane. This explains the slight undershoot at the beginning of the angular velocity response in Fig. 3.

Fig. 4 compares the robust angular velocity response of the sequential, iterative, and Aio strategies to uncertainty varying between 0% and 20%. The Aio and sequential strategies yielded improved robustness compared to the iterative. Fig. 5 compares the robust voltage response of the sequential, iterative, and Aio strategies to uncertainty varying between 0% and 20%. The Aio strategy maintains lower control effort compared to the sequential and iterative strategies.

B. Coupling Between Robust Design and Robust Control

Several authors have examined strength-based coupling between design and control systems with uncertainty not included in both systems [3], [7]. Reyer *et al.* [9] and Fathy *et al.* [11] proposed the use of optimality conditions to characterize coupling. They defined coupling relative to the solution method, for example, by comparing the optimality conditions of a sequential strategy with the optimality conditions of the Aio strategy.

Here, we also define coupling relative to the solution method by comparing the optimal worst case performance of the Aio strategy with the optimal worst case performance of the iterative strategy under uncertainty. Coupling in this paper is defined in terms of Aio and iterative strategies as opposed to Aio and sequential strategies because the sequential strategy solution is inconsistent. Because now uncertainty is included in both design and control systems, a relationship develops between coupling and the level of uncertainty applied. Such a relationship is important because designers could use this information to avoid performing costly optimizations.

Consider the following definition for the bound on uncertainty $\boldsymbol{\alpha}_{\bar{\mathbf{x}}} = \alpha(1.02, -1.02,\ 1.008, -1.008, 1.04, -1.04)^T$, where α is defined as the level of uncertainty. The level of uncertainty $\alpha \in [0, 1]$ is used to vary the uncertainty set for the RDRC problem. In addition, let F^*_{iter} represent the optimal worst case objective obtained using the iterative strategy and F^*_{all} represent the optimal worst case objective obtained using the Aio strategy. We now develop a definition for coupling strength based on the solution method.

For this definition, the coupling strength measure represents the absolute change between optimal worst case performances of iterative and Aio strategies $|F^*_{\mathrm{all}} - F^*_{\mathrm{iter}}|$. Zero coupling (uncoupled) means that solving the problem using the iterative strategy or using the Aio will result in the same optimal worst case objective $(F^*_{\mathrm{all}} = F^*_{\mathrm{iter}})$. If coupling is very small, then the Aio strategy optimal worst case objective will be slightly smaller than the iterative strategy optimal worst case objective. If coupling is high, then the Aio strategy optimal worst case objective will be much smaller than the iterative strategy optimal worst case objective. Since we know that the iterative strategy computational effort was lower compared to the Aio for nominal systems (zero uncertainty), then designers, in this case, should use the iterative strategy to save computational effort if the systems are uncoupled or coupling is very small.

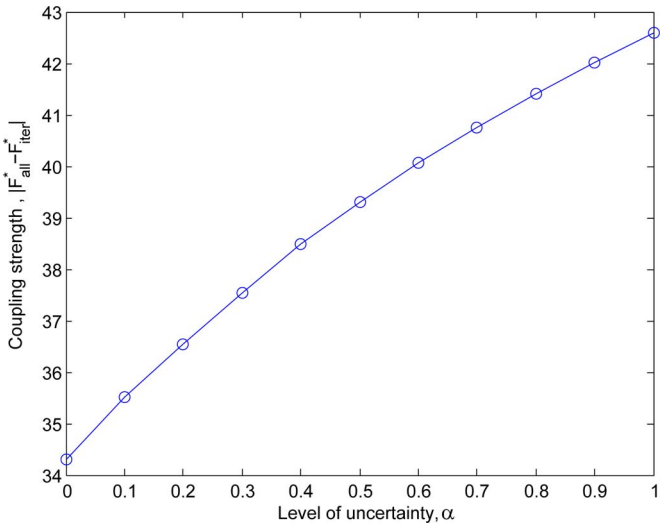

Fig. 6. Relationship between level of uncertainty and coupling defined relative to the iterative strategy.

Fig. 6 illustrates the relationship between design/control coupling and level of uncertainty α by comparing the difference between optimal worst case performances of the Aio and iterative strategies and level of uncertainty α. The absolute difference between optimal worst case performances of iterative and Aio strategies increases as the level of uncertainty α is increased. Hence, one can conclude that increasing the uncertainty level α tends to increase the coupling between robust design and robust control. Therefore, designers who demand more robustness should consider solving the RDRC because the iterative strategy will not necessarily improve robustness due to the coupling increase. Another important conclusion is that, in practice, good models (with low uncertainty) are needed to get good results with the iterative strategy.

VI. Conclusion and Future Work

This paper introduced a formulation that combined robust design with robust control. Several optimization strategies were proposed to solve this formulation and these strategies were illustrated on the RDRC of a dc motor as a case study.

The coupling between robust design and robust control is then related to the level of set-based parametric uncertainty applied. This relationship states that increasing the level of uncertainty increases coupling between robust design and robust control. Designers who demand more robustness should consider solving the RDRC because the iterative strategy will not necessarily improve robustness due to the coupling increase. Another important conclusion is that, in practice, good models (with low uncertainty) are needed to get good results with the iterative strategy. The impact of introducing uncertainty on the computational effort of different optimization strategies was then investigated. The iterative strategy required much more computational effort compared to the Aio and sequential strategies.

Future work should consider investigating the coupling relationship to uncertainty when other uncertainty representations (e.g., probabilistic or fuzzy) are used.

REFERENCES

[1] H. K. Fathy, P. Y. Papalambros, A. G. Ulsoy, and D. Hrovat, "Nested plant/controller optimization with application to combined passive/active automotive suspensions," in *Proc. Amer. Control Conf.*, Denver, CO, Jun. 4–6, 2003, vol. 4, pp. 3375–3380.

[2] B. Moulin, M. Idan, and M. Karpel, "Aeroservoelastic structural and control optimization using robust design schemes," *J. Guid. Control Dyn.*, vol. 25, pp. 152–159, 2002.

[3] J. Onoda and R. T. Haftka, "Approach to structure/control simultaneous optimization for large flexible spacecraft," *AIAA J.*, vol. 25, pp. 1133–1138, 1987.

[4] S. V. Savant and H. H. Asada, "Integrated structure/control design based on model validity and robustness margin," in *Proc. Amer. Control Conf.*, San Diego, CA, Jun. 2–4, 1999, vol. 4, pp. 2871–2875.

[5] L. Zollo, S. Roccella, E. Guglielmelli, M. C. Carrozza, and P. Dario, "Biomechatronic design and control of an anthropomorphic artificial hand for prosthetic and robotic applications," *IEEE/ASME Trans. Mechatronics*, vol. 12, no. 4, pp. 418–429, Aug. 2007.

[6] J. A. Reyer and P. Y. Papalambros, "Combined optimal design and control with application to an electric DC motor," *J. Mech. Des.*, vol. 124, pp. 183–191, 2002.

[7] G. P. O'Neal, B.-K. Min, Z. J. Pasek, and Y. Koren, "Integrated structural/control design of micro-positioner for boring bar tool insert," *J. Intell. Mater. Syst. Struct.*, vol. 12, pp. 617–627, 2001.

[8] A. C. Pil and H. H. Asada, "Integrated structure/control design of mechatronic systems using a recursive experimental optimization method," *IEEE/ASME Trans. Mechatronics*, vol. 1, no. 3, pp. 191–203, Sep. 1996.

[9] J. A. Reyer, H. K. Fathy, P. Y. Papalambros, and A. G. Ulsoy, "Comparison of combined embodiment design and control optimization strategies using optimality conditions," in *Proc. ASME Des. Eng. Tech. Conf.*, Pittsburgh, PA, Sep. 9–12, 2001, vol. 2, pp. 1023–1032.

[10] M. M. da Silva, O. Brüls, W. Desmet, and H. Van Brussel, "Integrated structure and control design for mechatronic systems with configuration-dependent dynamics," *Mechatronics*, vol. 19, no. 6, pp. 1016–1025, 2009.

[11] H. K. Fathy, J. A. Reyer, P. Y. Papalambros, and A. G. Ulsoy, "On the coupling between the plant and controller optimization problems," in *Proc. Amer. Control Conf.*, Arlington, VA, Jun. 25–27, 2001, vol. 3, pp. 1864–1869.

[12] H. Tanaka and T. Sugie, "General framework and BMI formulae for simultaneous design of structure and control systems," in *Proc. IEEE Conf. Decis. Control*, San Diego, CA, Dec. 10–12, 1997, vol. 1, pp. 773–778.

[13] H. S. Yan and G. J. Yan, "Integrated control and mechanism design for the variable input-speed servo four-bar linkages," *Mechatronics*, vol. 19, no. 2, pp. 274–285, 2009.

[14] G. Shi and R. E. Skelton, "An algorithm for integrated structure and control design with variance bounds," in *Proc. IEEE Conf. Decis. Control*, Kobe, Japan, Dec. 11–13, 1996, vol. 1, pp. 167–172.

[15] G. Shi, R. E. Skelton, and K. M. Grigoriadis, "An algorithm to integrate passive and active control," in *Proc. Joint Conf. Control Appl. Intell. Control Comput. Aided Control Syst. Des.*, Dearborn, MI, Sep. 15–18, 1996, vol. 1, pp. 536–541.

[16] M. Grossard, C. Rotinat-Libersa, N. Chaillet, and M. Boukallel, "Mechanical and control-oriented design of a monolithic piezoelectric microgripper using a new topological optimization method," *IEEE/ASME Trans. Mechatronics*, vol. 14, no. 1, pp. 32–45, Feb. 2009.

[17] M. Cakmakci and G. A. Ulsoy, "Improving component-swapping modularity using bidirectional communication in networked control systems," *IEEE/ASME Trans. Mechatronics*, vol. 14, no. 3, pp. 307–316, Jun. 2009.

[18] O. Gundogdu and K. Erenturk, "Fuzzy control of a DC motor driven four-bar mechanism," *Mechatronics*, vol. 15, pp. 423–438, 2005.

[19] A. M. Harb and I. A. Smadi, "Tracking control of DC motors via mimo nonlinear fuzzy control," *Chaos Solitons Fractals*, vol. 42, no. 2, pp. 702–710, 2009.

[20] Z. M. Al-Hamouz and H. N. Al-Duwaish, "New variable structure DC motor controller using genetic algorithms," in *Proc. IEEE Ind. Appl. Conf.*, St. Louis, MO, Oct. 12–15, 1998, vol. 3, pp. 1669–1673.

[21] H. Melkote and F. Khorrami, "Nonlinear adaptive control of direct-drive brushless DC motors and applications to robotic manipulators," *IEEE/ASME Trans. Mechatronics*, vol. 4, no. 1, pp. 71–81, Mar. 1999.

[22] K. Nouri, R. Dhaouadi, and N. B. Braiek, "Adaptive control of a nonlinear DC motor drive using recurrent neural networks," *Appl. Soft Comput.*, vol. 8, no. 1, pp. 371–382, 2008.

[23] G. G. Rigatos, "Adaptive fuzzy control of DC motors using state and output feedback," *Elect. Power Syst. Res.*, vol. 79, no. 11, pp. 1579–1592, 2009.

[24] D. U. Campos-Delgado and S. Martýnez-Martýnez, K. Zhou, "Integrated fault-tolerant scheme for a DC speed drive," *IEEE/ASME Trans. Mechatronics*, vol. 10, no. 4, pp. 419–427, Aug. 2005.

[25] S. E. Lyshevski, "Nonlinear control of mechatronic systems with permanent-magnet DC motors," *Mechatronics*, vol. 9, pp. 539–552, 1999.

[26] H. Grabner, W. Amrhein, S. Silber, and W. Gruber, "Nonlinear feedback control of a bearingless brushless DC motor," *IEEE/ASME Trans. Mechatronics*, vol. 15, no. 1, pp. 40–47, Feb. 2010.

[27] D. L. Peters, P. Y. Papalambros, and A. G. Ulsoy, "On measures of coupling between the artifact and controller optimal design problems," presented at the Int. Des. Eng. Tech. Conf. (DETC 2009)-86868, San Diego, CA, Aug. 30–Sep. 2, 2009.

[28] E. Hamdi, *Design of Small Electrical Machines*. West Sussex, U.K.: Wiley, 1994.

Sulaiman F. Alyaqout received the B.S. degree from Kuwait University, Safat, Kuwait, in 1999, and the M.S. and Ph.D. degrees from The University of Michigan, Ann Arbor, in 2003 and 2006, respectively, all in mechanical engineering.

He is currently an Assistant Professor of mechanical engineering in the Department of Mechanical Engineering, Kuwait University. His research interests include the dynamics and control of mechanical systems and systems optimization.

Panos Y. Papalambros received the diploma degree from the National Technical University of Athens, Athens, Greece, and the M.S. and Ph.D. degrees from Stanford University, Stanford, CA.

He is currently the Donald C. Graham Professor of Engineering and a Professor of mechanical engineering at The University of Michigan, Ann Arbor. He is also a Professor of architecture, and a Professor of art and design. He is the coauthor of *Principles of Optimal Design: Modeling and Computation* (Cambridge Univ. Press, 2000). His research interests include design science and systems optimization, with applications to product design and automotive systems.

Dr. Papalambros is a Fellow of the American Society of Mechanical Engineers (ASME) and the Society of Automotive Engineers. He was the recipient of the ASME Design Automation Award in 1998, the ASME Machine Design Award in 1999, the Japan Society of Manufacturing Engineers Design and Systems Achievement Award in 2004, and the ASME Joel and Ruth Spira Outstanding Design Educator Award in 2007.

A. Galip Ulsoy received the B.S. degree from Swarthmore College, Swarthmore, PA, in 1973, the M.S. degree from Cornell University, Ithaca, NY, in 1975, and the Ph.D. degree from the University of California, Berkeley in 1979.

He is currently the C.D. Mote, Jr., Distinguished University Professor of Mechanical Engineering and the William Clay Ford Professor of Manufacturing at The University of Michigan, Ann Arbor. His research interests include the dynamics and control of mechanical systems.

Dr. Ulsoy has received numerous awards, including the American Automatic Control Council's 1993 O. Hugo Schuck Best Paper Award, the 2003 Rudolf Kalman Best Paper Award from the *Journal of Dynamic Systems, Measurement and Control*, the 2008 Albert M. Sargent Progress Award from the Society of Manufacturing Engineers (SME), and the 2008 Rufus T. Oldenburger Medal from the American Society of Mechanical Engineers (ASME). He is a member of the National Academy of Engineering and a Fellow of both the American Society of Mechanical Engineers (ASME) and the Society of Manufacturing Engineers (SME).